Lepto-hadronic model for the broadband emission of Cygnus X-1: preliminary results

C. Pepe[1], G.S. Vila[1] & G.E. Romero[1, 2]

[1] *Instituto Argentino de Radioastronomía (IAR - CONICET)*
[2] *Facultad de Ciencias Astronómicas y Geofísicas (UNLP)*

Contact/ CP: carolina@iar.unlp.edu.ar

Resumen / Distintos autores han enfocado sus esfuerzos en explicar la emisión del microcuásar Cygnus X-1 a través del desarrollo de modelos radiativos para el jet. Sin embargo, se han considerado solo modelos leptónicos a pesar de que la presencia de protones en el *jet* permitiría explicar algunas características de la emisión de altas energías en esta fuente, y de que existe fuerte evidencia de contenido hadrónico en los jets de otras binarias de rayos X. En este trabajo se presenta la aplicación de un modelo lepto-hadrónico para el espectro electromagnético multifrecuencia de Cyg X-1. En dicho modelo, la inyección de partículas relativistas ocurre en una región extendida del jet y se calcula su contribución al espectro electromagnético a través de varios procesos radiativos. Además, se incluye la contribución de las partículas secundarias (piones, muones y pares electrón-positrón) así como los efectos de autoabsorción de los fotones creados en el jet. Por último, se estudian los aspectos radiativos de la interacción del viento de la estrella compañera con el jet.

Abstract / Different authors have made efforts to explain the emission of the microquasar Cygnus X-1 by means of radiative models for the jet. However, so far, only leptonic models have been considered despite the fact that the presence of protons in the jet would explain some features of the high-energy emission of this source. Additionally, there is strong evidence of hadronic content in the jets of other X ray binaries. In this work we present the application of a lepto-hadronic model to the broadband electromagnetic spectrum of Cyg X-1. In such model, the injection of relativistic particles occurs in an extended region of the jet and we calculate the contribution of all particles species (including secondary particles) to the jet emissivity by several radiative process. Also, the effects of self-absortpion due to the photons created inside the jet itself are considered as well as the radiative output due to the interaction between the jet and the wind of the donor star.

Keywords / black hole physics — relativistic processes — radiation mechanisms: non-thermal

1. Introduction

Cygnus X-1 is the Galactic X-ray binary with the highest probability of hosting a black hole. The system is composed of a black hole candidate of 14.8 $M_\odot$ and a high-mass stellar companion of $\sim 20\ M_\odot$ (Orosz et al., 2011). Being most of the time in the hard spectral state, Cyg X-1 has been observed in a wide range of the electromagnetic spectrum (for a compilation of the data see Zdziarski et al., 2014).

As far as content is concerned, the presence of a non-thermal leptonic component in the jets of microquasars is generally approved. However, hadrons have only been detected in two microquasars: SS 433 (Migliari et al., 2002) and 4U 1630C47 (Díaz Trigo et al., 2013). In the case of Cyg X-1, from the study of the effects of the jet in the interstellar medium it has been suggested that the jet should carry a significant amount of energy in cold protons (Gallo et al., 2005). Furthermore, since there seems to exist a correlation between the accretion and ejection of matter in microquasars (Mirabel et al., 1998), assuming the same composition for accreted and ejected matter would be a reasonable guess. Hence, the presence of protons in the jets of microquasars appears quite likely.

In this work, we apply and extend the model developed in Vila et al. (2012). In this scenario, the jet is composed of both, leptons and hadrons. They are injected in an spatially extended and inhomogeneous region of the jet and the effects of propagation and cooling of these particles on the radiative output is considered. In addition to the several radiative process considered in that previous work, the interaction between the relativistic particles and the radiation and matter fields of the stellar companion are also taken into account since, unlike low-mass X-ray binaries, in Cyg X-1 it is a massive and evolved star with strong winds. All the secondary particles injected by the internal and external cooling processes of the primary particles also contribute to the radiative output of the source. In section 2. we summarize the main features of the model of Vila et al. (2012). The reader is referred to this article for details on the calculations. Finally, in section 3. we present our results and summarize our conclusions.

2. The model

2.1. Basic scenario

The jet model we adopt is extensively described in Vila et al. (2012). In Fig. 1 we show a basic sketch of both, the binary system and the jet. The massive companion star is located 3.2×10^{12} cm away from the black hole. With a termination wind velocity of 2500 km s^{-1}, it is an important source of matter and radiation. The jet is launched perpendicularly to the accretion disk at a distance z_0 from the black hole and propagates up to $z_{\rm end}$. It is assumed that a diffusive shock acceleration mechanism operates on the relativistic particles⋆. Table 1 summarizes the relevant parameters of the model.

BH mass ($M_{\rm BH}$)	27 $M_\odot$
Orbital separation ($a_\bigstar$)	3.2×10^{12} cm
Star temperature ($T_\bigstar$)	2.8×10^4 K
Terminal wind velocity (v_∞)	2500 km s^-1
Star mass loss rate ($\dot{M}_\bigstar$)	10^5 $M_\odot$ yr^{-1}
Penetration factor (χ)	0.105
Jet bulk Lorentz factor ($\Gamma_{\rm bulk}$)	1.25
Spectral Index (Γ)	1.8
Acceleration efficiency (η)	0.07
Begin acceleration region ($z_{\rm acc}$)	6×10^8 cm
End acceleration region ($z_{\rm max}$	5×10^{13} cm
Protons to leptons power ratio (a)	80

Table 1: Relevant parameters of the model.

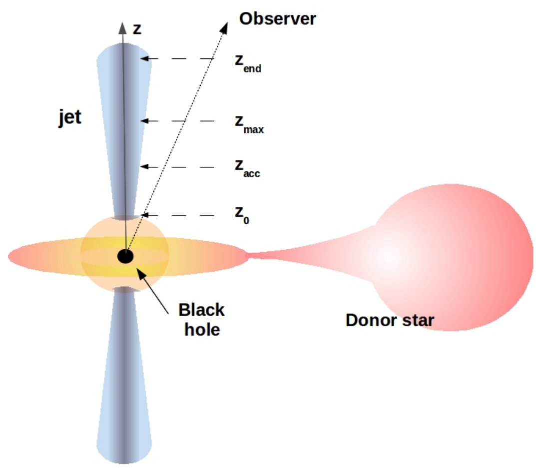

Fig. 1: Basic sketch of the microquasar. Details of the jet and the acceleration region (not to scale) are also shown.

2.2. Radiative processes and particle cooling

Several processes contribute to the particle cooling since they can interact with the magnetic, radiation and matter fields. The cooling rate for the process i is defined as

$$t_i^{-1} = -\frac{1}{E}\frac{dE}{dt}|_i, \tag{1}$$

where E is the particle energy. The synchrotron, Bremstrahlung and inverse Compton (IC) cooling rates for leptons in the jet interacting with both, magnetic field and low-energy radiation, respectively, are detailed in Vila et al. (2012). The synchrotron radiation of primary electrons provides the target field for internal IC. Note that all secondary leptons cool via these three processes. IC scattering between relativistic leptons and low-energy photons radiated from the accretion disk is also considered. On the other hand, protons cool via proton-photon and proton-proton interactions, injecting pions in the jet. The decay of neutral pions, subsequently, injects photons while the charged pions inject electron-positron pairs and neutrinos⋆⋆. The cross-section of pion-proton interactions is $\sim 2/3$ of that for proton-proton collisions Gaisser (1990) and the same approximation is applied for pion-photon collisions. All cooling rates are calculated in the jet frame except the proton-proton cooling rate, for which calculations are simpler in the observer frame (Vila et al., 2012). Since the stellar photon distribution is not isotropic in the jet frame, we must use the full cross sections whenever necessary. The treatment of the interaction with the low-energy photons coming from the companion star follows that of Vila et al. (2012) for the accretion disk. To this purpose, we assume the star radiates as a black body of $T_\bigstar = 2.8 \times 10^4$ K. On the other hand, as the proton-proton cooling rate is calculated in the observer frame, we only need to estimate the stellar wind density. This is achieved by means of the continuity equation

$$\dot{M} = 4\Pi r^2 \rho(r) v(r), \tag{2}$$

where r is the distance to the center of the star, and ρ and v, its density and velocity, respectively. Since the velocity profile for massive stars is known (Lamers & Cassinelli, 1990), the particle density profiles results,

$$n(z) = \frac{\dot{M}_\bigstar}{4\pi(a_\bigstar^2 + z^2)v_\infty m_p}\left(1 - \frac{R_\bigstar}{\sqrt{a_\bigstar^2 + z^2}}\right)^{-1}, \tag{3}$$

where $a_\bigstar$ is the binary separation, $R_\bigstar$ the star radius, $\dot{M} = 1 \times 10^{-5}$ $M_\odot$ is the mass loss rate of the companion star and z is the distance along the jet to the black hole. We account for the mixing of the jet-wind system by means of a phenomenological penetration factor of the wind into the jet, χ (the estimation of this parameter is based on the simulations of Perucho et al., 2010). Finally, photomeson production is not considered because the stellar photons do not have enough energy to reach the threshold energy of this process and, for the same reason, photopair production is neglected since it does not contribute significantly to the radiative output of the jet.

⋆ The acceleration rate depends on an acceleration efficiency parameter, η.

⋆⋆ However, we do not include the treatment of the evolution of neutrinos in this work. See Reynoso & Romero (2009) for a work on this subject.

2.3. Distribution of particles

The injection function of primary electrons and protons is parametrized as a power-law in energy multiplied by an exponential cutoff

$$Q(E,z) = Q_0 E^{-\Gamma} \exp[-E/E_{\max}(z)] f(z). \quad (4)$$

The cutoff energy $E_{\max}$ is calculated by balancing the energy-loss rate and the acceleration rate and it depends on the height z. The step-like function $f(z)$ accounts for the acceleration region extension

$$f(z) = 1 - \frac{1}{1+\exp[-(z - z_{\max})]}. \quad (5)$$

Finally the value of the normalization constant Q_0 is obtained from the total power injected in each particle species. The power injected in relativstic protons and electrons are related as $L_p = aL_e$, with a a free parameter. See the references in Vila et al. (2012) for the complete expresions of the injection function of secondary particles.

Once the injection function is known, we calculate the isotropic, steady-state particle distribution $N(z)$ in the jet reference frame by solving a transport equation of the form (e.g. Khangulyan et al., 2008)

$$v_{\rm conv}\frac{\partial N}{\partial E} + \frac{\partial}{\partial E}\left(\frac{dE}{dt}|_{\rm tot} N\right) + \frac{N}{\tau_{\rm dec}(E)} = Q(E,z), (6)$$

where $v_{\rm conv} \sim v_{\rm jet}$ is the convection velocity and $\tau_{\rm dec}(E)$ is the mean lifetime of decaying particles. From left to right, the three terms in Eq. 6 account for the changes in $N(E,z)$ caused by particle convection along the jet, energy losses and decay.

3. Results and conclusions

We calculate the radiative spectrum of all particle species produced by the interaction processes described in Section 2.2.. The spectra are first obtained in the comoving frame and then transformed to the observer frame whenever necessary (see Vila et al., 2012, for details). The emission spectrum must be corrected for absorption caused by photon-photon annihilation

$$\gamma + \gamma \rightarrow e^+ + e^-. \quad (7)$$

To this aim, two different target fields of low-energy photons are considered: the isotropic synchrotron radiation from primary electrons and the beamed stellar radiation. The latter is the dominant absorption effect up to distances of order of $\sim a_\bigstar$. Because of the non-isotropic nature of this radiation field, special considerations regarding the geometry have been taken into account.

In Fig. 2 we show the resulting spectrum for the parameters listed in Table 1. These result as the best-fit parameters from a wide scanning of parameter values. In addition to the radiative processes listed in Section 2.2., the star, disk and corona luminosity are also calculated. The radio emission of the jet is synchrotron radiation although it does not quite explain the MeV tail

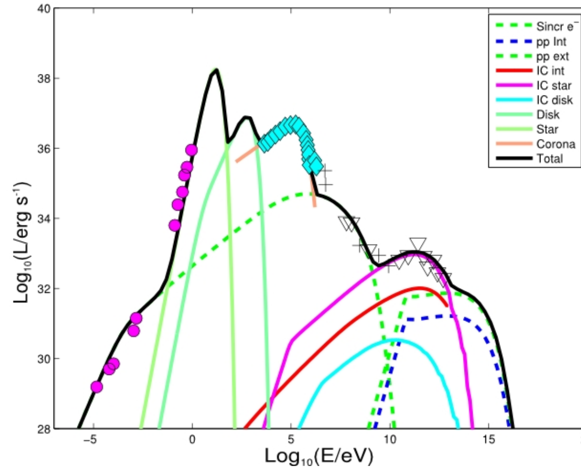

Fig. 2: Best-fit spectral energy distribution for the broadband data of Cygnus X-1. The data are taken from the references listed inZdziarski et al. (2014).

of the spectrum (see Romero et al., 2014, for a different origin of this emission). The dominant channel for IC emission is the interaction with the low-energy stellar photons. This highlights the need to include such a target field for a comprehensive model. Although most of the energy is transferred to relativistic protons ($a = 80$), the hadronic contribution to the spectrum is not significant up to $\sim TeV$. However, the proton-proton luminosities (internal and external) are responsible for the ultra-high energy emission of the source. This is also consequence of the effective mixing of the jet-wind system ($\chi \sim 0.105$) which strongly constraints the dynamics of the jet-wind interface. Nonetheless, dynamical considerations are left for forthcoming works.

In this work we present an inhomogeneous model for the broadband emission of high-mass microquasars. The main difference with the model developed in Vila et al. (2012) is the interaction with both, the radiation and matter fields of the companion star. The model was applied to the source Cygnus X-1. For the first time, a hadronic model is applied to this source and it predicts that *pp* interactions can explain the still undetected ultra-high energy emission of this source.

References

Díaz Trigo M., et al., 2013, Nature, 504, 260
Gaisser T. K., 1990, Cosmic rays and particle physics
Gallo E., et al., 2005, Nature, 436, 819
Khangulyan D., Aharonian F., Bosch-Ramon V., 2008, MNRAS, 383, 467
Lamers H. J. G. L. M., Cassinelli J. P., 1990, Introduction to stellar winds
Migliari S., Fender R., Méndez M., 2002, Science, 297, 1673
Mirabel I. F., et al., 1998, A&A, 330, L9
Orosz J. A., et al., 2011, ApJ, 742, 84
Perucho M., Bosch-Ramon V., Khangulyan D., 2010, A&A, 512, L4
Reynoso M. M., Romero G. E., 2009, A&A, 493, 1
Romero G. E., Vieyro F. L., Chaty S., 2014, A&A, 562, L7
Vila G. S., Romero G. E., Casco N. A., 2012, A&A, 538, A97

Zdziarski A. A., et al., 2014, MNRAS, 442, 3243